MolecularMedicine

Supplemental Data

Reduction of Cardiac Cell Death after Helium Postconditioning in Rats: Transcriptional Analysis of Cell Death and Survival Pathways

Gezina TML Oei,[1] Michal Heger,[2] Rowan F van Golen,[2] Lindy K Alles,[2] Moritz Flick,[1] Allard C van der Wal,[3] Thomas M van Gulik,[2] Markus W Hollmann,[1] Benedikt Preckel,[1] and Nina C Weber[1]

Online address: http://www.molmed.org

The Feinstein Institute for Medical Research
Empowering Imagination. Pioneering Discovery.®
North Shore LIJ

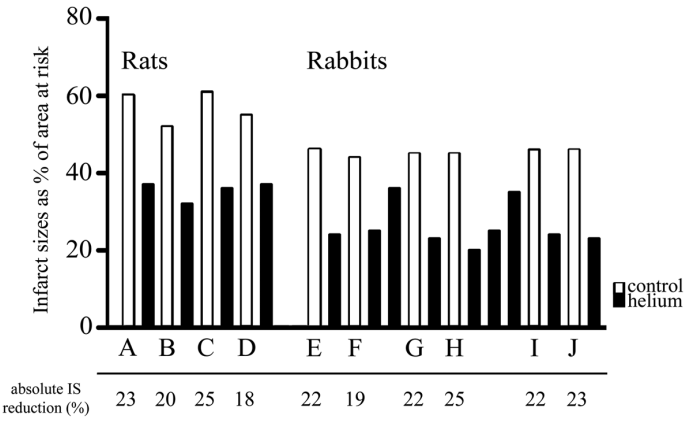

Supplementary Figure S1. Literature overview of infarct size reduction after helium preconditioning. Summary of literature in which infarct sizes are plotted as a percentage of area at risk after helium preconditioning. Data are plotted as means. At the bottom of the figure an overview of the absolute infarct size reduction is given. Infarct size reduction by early preconditioning (EPC) entails application of 5-min cycles of helium inhalation before the ischemic episode. EPC1, EPC3 and EPC5 consist of 1, 3 or 5 5-min cycles of helium before ischemia, respectively. Late preconditioning (LPC) is based on 15 min of helium administration 24 h before the ischemic episode and also results in infarct size reduction. Rat experiments: 25 min of ischemia and 2 h of reperfusion, rabbit experiments 30 min of ischemia and 3 h of reperfusion. A (1): n=8 per group, EPC3; B (2): n=8 per group, EPC3; C (3): n=10 per group, EPC3; D (4): n=8-12 per group, LPC; E (5): n=6 per group, EPC3; F (6): n=6/7 per group, EPC3, EPC1; D (7): n=7/8 per group, EPC3; G (8): n=6/7 per group, EPC5, EPC3, EPC1; H (9): n=8 per group, EPC3; I (10): n=8 per group, EPC3.

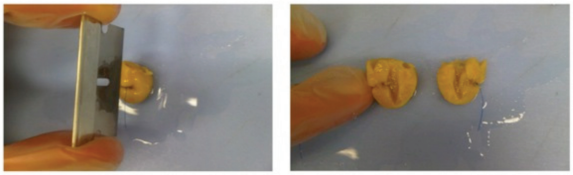

Supplementary Figure S2. Preparation of histological slices. Hearts were cut in two parts, crossing the previous ligation of the LAD.

Supplementary Table S1. RNA extraction, cDNA synthesis and run parameters.

Program name	Target (°C)	Acquisition Mode	Hold (hh:mm:ss)	Ramp Rate (°C/s)	Acquisition (per °C)	Sec Target (°C)	Step Size (°C)	Step Delay (cycles)	Cycles	Analysis mode
Heat activation	95	none	00:10:00	4.4		0	0	0		
PCR cycle	95	none	00:00:15	1.0		0	0	0	50	quantification
	60	single	00:01:00	1.0		0	0	0		
Melting curves	60	none	00:00:15	4.4						
	95	continuous		0.03	20					

RNA was extracted from heart tissue using the RNAeasy Fibrous Tissue Mini Kit (Qiagen, Venlo, The Netherlands) according to manufacturer's instructions. All materials and reagents used in the procedure were from Qiagen, unless stated otherwise. In brief, ±30 mg of heart tissue was added to 300 μL of RLT lysis buffer containing 1% (v/v) β-mercaptoethanol and homogenized with a MagNA Lyser using MagNA Lyser Green Beads (both from Roche Applied Sciences, Penzberg, Germany). The lysate was collected and 600 μL of nuclease-free water containing 1.67% (v/v) proteinase K was added to digest residual fibrous tissue (6 min at 55°C). Total RNA was extracted using spin columns, including on-column DNAse I treatment, and eluted in 30 μL of nuclease-free water. Next, eluate RNA concentrations were determined by UV-vis absorbance spectroscopy (NanoDrop, Thermo Scientific, Rockford IL). RNA yields typically ranged from 0.3 to 3 μg/μL (data not shown). To ensure RNA purity, samples with an A260/A280 ratio of ≤1.99 were excluded from further analysis.

Next, 1 μg of RNA was reverse transcribed to cDNA. using the RT^2 First Strand Kit according to manufacturer's instructions. RNA was reverse transcribed to cDNA using the RT^2 First Strand Kit (Qiagen, catalogue number #330401) according to manufacturer's instructions. Before starting the procedure, the RNA concentration of all samples was diluted to 250 ng/μL with nuclease-free water. Next, 1 μg (4 μL) of RNA was mixed with 2 μL of GE-buffer and 2 μL of nuclease-free water and incubated at 42°C for 5 min to eliminate any residual DNA. Following incubation at 4°C (1 min), 10 μL of reverse transcriptase mix was added to each 10 μL sample and reverse transcription was started by incubating the samples at 42°C for 15 min and subsequently terminated by raising the temperature to 92°C for 5 min. Last, 91 μL of nuclease-free water was added to each sample.

For optimal temperature control, cDNA synthesis was performed on a PTC-200 thermal cycler (MJ Research, Waltham, MA). cDNA was subsequently mixed with RT^2 SYBR Green qPCR Mastermix and nuclease-free water according to the manufacturer's instructions, loaded (25 μL/well) onto the Rat Cell Death PathwayFinder PCR Array (SABiosciences catalogue number #PARN-212A), and run on a LightCycler 480 (Roche Applied Sciences).

Supplementary Table S2. Gene descriptions.

Gene abbreviation	Category	Gene Description	Gene name
Abl1	pro-apoptosis	C-abl oncogene 1, **non-** receptor tyrosine kinase	Abl
Akt1	anti-apoptosis, autophagy	V-akt murine thymoma viral oncogene homolog 1	Akt
Apaf1	pro-apoptosis	Apoptotic peptidase activating factor 1	-
App	autophagy	Amyloid beta (A4) precursor protein	-
Atg12	autophagy	ATG12 autophagy related 12 homolog (S. cerevisiae)	Apg12l, MGC125080
Atg16l1	autophagy	ATG16 autophagy related 16-like 1 (S. cerevisiae)	Apg16l, Wdr30
Atg3	autophagy	ATG3 autophagy related 3 homolog (S. cerevisiae)	Apg3l, PIG-1, Pig1
Atg5	autophagy	ATG5 autophagy related 5 homolog (S. cerevisiae)	-
Atg7	autophagy	ATG7 autophagy related 7 homolog (S. cerevisiae)	Apg7l
Atp6v1g2	necrosis, pro-apoptosis	ATPase, H+ transporting, lysosomal V1 subunit G2	ATP6G, Atp6g2, NG38
Bax	pro-apoptosis, autophagy	Bcl2-associated X protein	-
Bcl2	anti-apoptosis, autophagy	B-cell CLL/lymphoma 2	Bcl-2
Bcl2a1d	anti-apoptosis	B-cell leukemia/lymphoma 2 related protein A1d	Bcl2a1
Bcl2l1	anti-apoptosis, autophagy	Bcl2-like 1	Bcl-xl, Bcl2l, Bclx, bcl-X
Bcl2l11	pro-apoptosis	BCL2-like 11 (apoptosis facilitator)	Bim, BimL
Becn1	autophagy	Beclin 1, autophagy related	-
Birc2	anti-apoptosis (11)	Baculoviral IAP repeat-containing 2	Api2, rIAP1
Birc3	anti-apoptosis	Baculoviral IAP repeat-containing 3	Birc2, IAP1, MGC93416
Bmf	necrosis	Bcl2 modifying factor	-
Casp1	pro-apoptosis	Caspase 1	Ice, Il1bc
Casp2	anti-apoptosis/proapoptosis	Caspase 2	-
Casp3	pro-apoptosis, autophagy	Caspase 3	Lice, MGC93645

Continued on next page

Supplementary Table S2. ***Continued.***

Casp6	pro-apoptosis	Caspase 6	MGC93335, Mch2
Casp7	pro-apoptosis	Caspase 7	-
Casp9	pro-apoptosis	Caspase 9, apoptosis-related cysteine peptidase	Apaf3, Casp-9-CTD, Casp9_v1, Ice-Lap6, Mch6
Cd40	pro-apoptosis	CD40 molecule, TNF receptor superfamily member 5	Tnfrsf5
Cd40lg	pro-apoptosis	CD40 ligand	Tnfsf5
Cflar	pro-apoptosis?	CASP8 and FADD-like apoptosis regulator	Flip, MGC108616
Commd4	necrosis	COMM domain containing 4	-
Ctsb	autophagy	Cathepsin B	-
Ctss	autophagy	Cathepsin S	-
Cybb	necrosis	Cytochrome b-245, beta polypeptide	Gp91-phox, Nox2
Cyld	necrosis, pro-apoptosis	Cylindromatosis (turban tumor syndrome)	LRRGT00003, Rp1, Rp1h
Defb1	necrosis	Defensin beta 1	-
Dffa	Anti-apoptosis (12)	DNA fragmentation factor, alpha subunit	ICAD-S
Dpysl4	necrosis	Dihydropyrimidinase-like 4	Crmp3, Dpys4
Esr1	autophagy	Estrogen receptor 1	ER-alpha, Esr, RNESTROR
Fas	pro-apoptosis, autophagy	Fas (TNF receptor superfamily, member 6)	Tnfrsf6
Faslg	pro-apoptosis	Fas ligand (TNF superfamily, member 6)	Apt1Lg1, CD95-L, Fasl, Tnfsf6
Foxi1	necrosis	Forkhead box I1	-
Gaa	autophagy	Glucosidase, alpha, acid	MGC72625
Gadd45a	pro-apoptosis	Growth arrest and DNA-damage-inducible, alpha	Ddit1, Gadd45
Galnt5	necrosis	UDP-N-acetyl-alpha-D-galactosamine:polypeptide N-acetylgalactosaminyltransferase 5 (GalNAc-T5)	-
Grb2	necrosis	Growth factor receptor bound protein 2	MGC108668
Hspbap1	necrosis	Hspb associated protein 1	Pass1
Htt	autophagy	Huntingtin	Hd, Hdh
Ifng	autophagy	Interferon gamma	IFNG2
Igf1	autophagy	Insulin-like growth factor 1	-
Igf1r	anti-apoptosis	Insulin-like growth factor 1 receptor	IGFIRC, JTK13
Ins2	autophagy	Insulin 2	-
Irgm	autophagy	Immunity-related GTPase family, M	Ifi1
Kcnip1	necrosis	Kv channel-interacting protein 1	Kchip1
Map1lc3a	autophagy	Microtubule-associated protein 1 light chain 3 alpha	MGC105263
Mapk8	autophagy	Mitogen-activated protein kinase 8	JNK
Mcl1	anti-apoptosis/proapoptose	Myeloid cell leukemia sequence 1	-
Nfkb1	autophagy	Nuclear factor of kappa light polypeptide gene enhancer in B-cells 1	NF-kB
Nol3	anti-apoptosis (13)	Nucleolar protein 3 (apoptosis repressor with CARD domain)	Arc
Olr1583	necrosis	Olfactory receptor 1583	-
Parp2	necrosis	Poly (ADP-ribose) polymerase 2	Adprtl2
Pik3c3	autophagy	Phosphoinositide-3-kinase, class 3	-
Pten	autophagy	Phosphatase and tensin homolog	MMAC1, Mmac, TEP1
Pvr	necrosis	Poliovirus receptor	Taa1, Tage4
Rab25	necrosis	RAB25, member RAS oncogene family	-
RGD1311517	necrosis	Similar to RIKEN cDNA 9430015G10	-
RGD1562639	necrosis	Similar to c-myc promoter binding protein	-
Rps6kb1	autophagy	Ribosomal protein S6 kinase, polypeptide 1	-
Snca	autophagy	Synuclein, alpha (non A4 component of amyloid precursor)	MGC105443
Spata2	necrosis, pro-apoptosis?	Spermatogenesis associated 2	MGC93291
Sqstm1	autophagy	Sequestosome 1	Osi, ZIP, ZIP3
Sycp2	necrosis, pro-apoptosis?	Synaptonemal complex protein 2	-
Tmem57	necrosis	Transmembrane protein 57	MGC116145
Tnf	pro-apoptosis, autophagy	Tumor necrosis factor (TNF superfamily, member 2)	MGC124630, RATTNF, TNF-alpha, Tnfa
Tnfrsf10b	pro-apoptosis	Tumor necrosis factor receptor superfamily, member 10b	-
Tnfrsf11b	anti-apoptosis	Tumor necrosis factor receptor superfamily, member 11b	MGC93568, Opg
Tnfrsf4	necrosis	Tumor necrosis factor receptor superfamily, member 4	Ox40, Txgp1
Tnfrsf8	necrosis	Tumor necrosis factor receptor superfamily, member 8	Cd30
Tp53	pro-apoptosis, autophagy	Tumor protein p53	MGC112612, Trp53, p53
Traf2	anti-apoptosis	Tnf receptor-associated factor 2	-
Txnl4b	necrosis	Thioredoxin-like 4B	MGC109322, RGD1305127
Ulk1	autophagy	Unc-51 like kinase 1 (C. elegans)	-
Xiap	anti-apoptosis	X-linked inhibitor of apoptosis	Api3, Birc4, riap3

METHODS: WESTERN BLOT ANALYSIS

Preparation of Cytosol, Membrane and Mitochondrial fractions

Excised hearts were shock-frozen in liquid nitrogen and pulverized in a precooled mortar. Samples were dissolved in lysis buffer containing Tris base, EGTA, NaF and Na_3VO_4 (as phosphatase inhibitors), an inase-inhibitor mix (aprotinin, leupetin and Pepsatin), DTT and okadaic acid. The solution was homogenized on ice (Homogenisator, Ultra-Turrax T8) and centrifuged slowly at 1000 g, 4°C for 10 min. The remaining supernatant was pipetted in new vials and centrifuged at 10000 g, from which a pellet remained containing the mitochondria. The supernatant was re-centrifuged at 12000 g to obtain a cytosolic fraction. The remaining pellet was suspended in lysis buffer (containing 1% Triton X-100), incubated for 60 min on ice and vortexed. The solution was centrifuged at 16000 g for 15 min, resulting in a supernatant containing the membrane fraction. All fractions were stored at -80°C.

Western Blot Analysis

After protein determination by the Bradford method (14), equal amounts of protein were mixed with sample buffer (containing SDS, Bromophenol Blue,Tris Base, Glycerol and Mercaptoethanol). Samples were vortexed, boiled at 95°C for 5 min, and loaded on a Criterion Gel. Proteins were separated by electrophoresis and transferred onto Immobilin-FL Membrane. Unspecific binding of the antibody was blocked by incubation with Odyssey® Blocking Buffer for 60 min. Subsequently, the membrane was incubated over night at 4°C with Beclin1 (Cell Signaling Technology, 1:1000) or Sequestosome1 (Abcam, 1:2000) antibody. After washing in fresh, cold TBS-T, the blot was subjected to the appropriate horseradish peroxidase conjugated secondary antibody for 1 h at room temperature, subsequently, immunoreactive bands were visualized by the Odyssey® Infrared Imaging System. The Odyssey® Infrared Scanning Software was used for quantification of the blots. Results are presented as the ratio of the target protein over the fraction-specific control protein: for the cytosol fraction this was actin (1:5000), for the membrane fraction NaKATPase (Cell Signaling Technology, 1:5000) and for the mitochondrial fraction AntiPHB1 (Cell Signaling Technology, 1:10000).

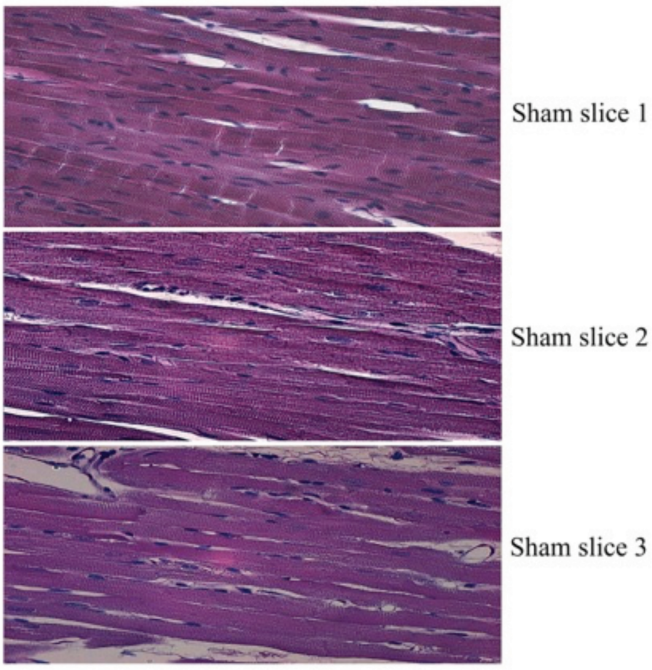

Supplementary Figure S3. Histology – Sham. Representative slices of three sham animals, 200 times enlarged. The pictures clearly show normally structured cardiomyocytes without edema or signs of cell damage.

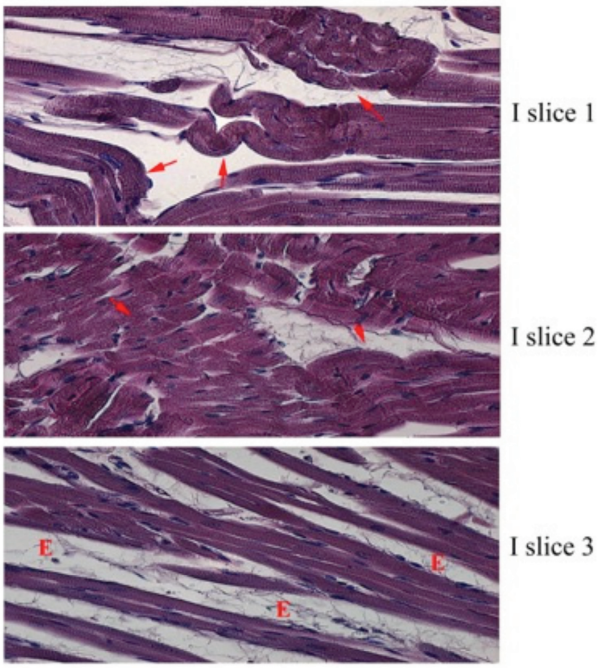

Supplementary Figure S4. Histology – Ischemia. Representative slices of three animals that underwent 25 min of ischemia, 200 times enlarged. Arrows indicate ischemic hypercontracture, E indicates edema.

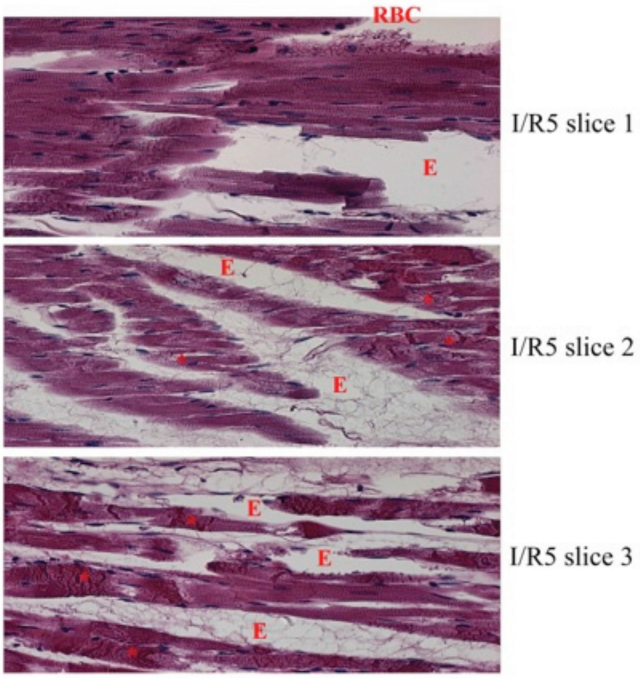

Supplementary Figure S5. Histology – I/R5. Representative slices of three animals that were exposed to 25 min of ischemia and 5 min of reperfusion, 200 times enlarged. E indicates edema, RBC indicates extravasation of red blood cells and asterisk indicates contraction band necrosis.

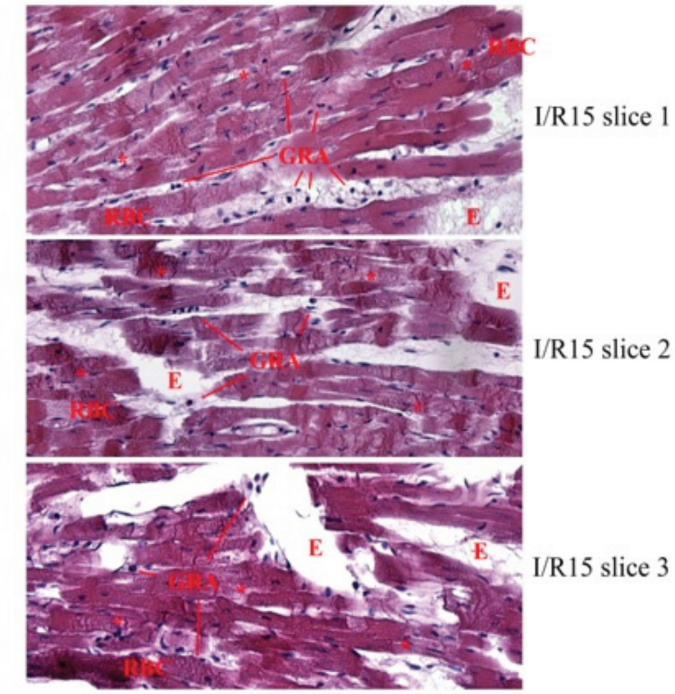

Supplementary Figure S6. Histology – I/R15. Representative slices of three animals that were exposed to 25 min of ischemia and 15 min of reperfusion, 200 times enlarged. E indicates edema, RBC indicates extravasation of red blood cells, GRA indicates extravasation of granulocytes and asterisk indicates contraction band necrosis.

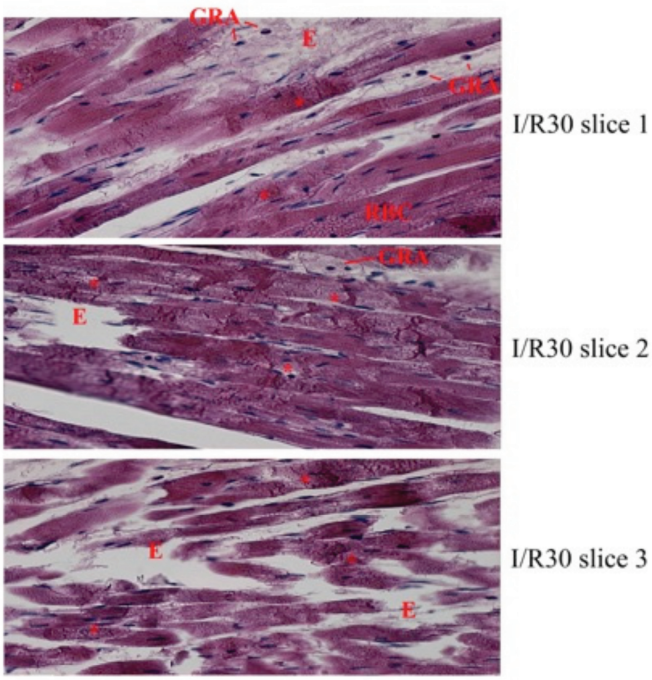

Supplementary Figure S7. Histology – I/R30. Representative slices of three animals that were exposed to 25 min of ischemia and 30 min of reperfusion, 200 times enlarged. E indicates edema, RBC indicates extravasation of red blood cells, GRA indicates extravasation of granulocytes and stars indicate contraction band necrosis.

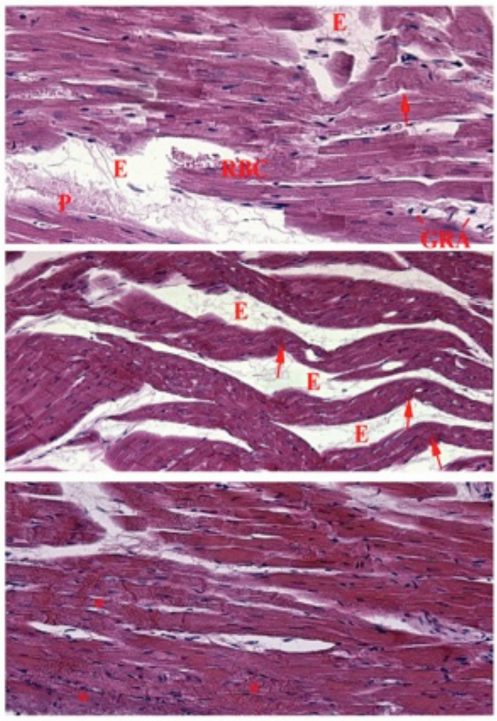

Supplementary Figure S8. Histology – He5. Representative slices of three animals that were exposed to 25 min of ischemia and 5 min of reperfusion with helium postconditioning for 5 min, 200 times enlarged. Arrows indicate hypercontracture, E indicates edema, RBC indicates extravasation of red blood cells, GRA indicates extravasation of granulocytes, P indicates presence of platelets and thrombi and asterisk indicates contraction band necrosis.

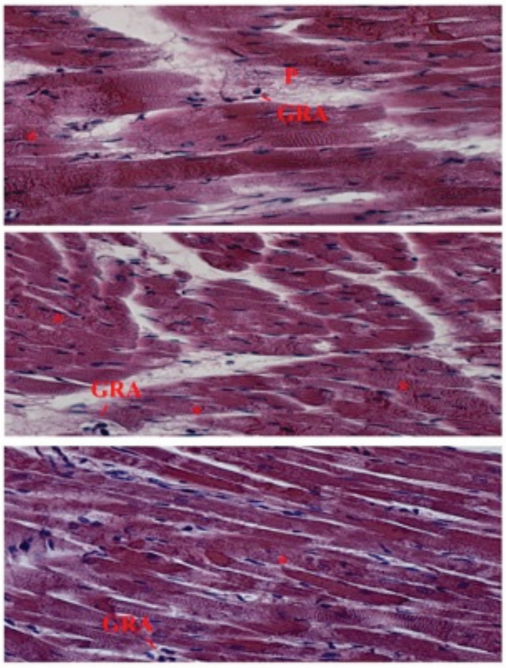

Supplementary Figure S9. Histology – He15. Representative slices of three animals that were exposed to 25 min of ischemia and 15 min of reperfusion with helium postconditioning for 15 min, 200 times enlarged. GRA indicates extravasation of granulocytes, P indicates presence of platelets and thrombi, and asterisk indicates contraction band necrosis.

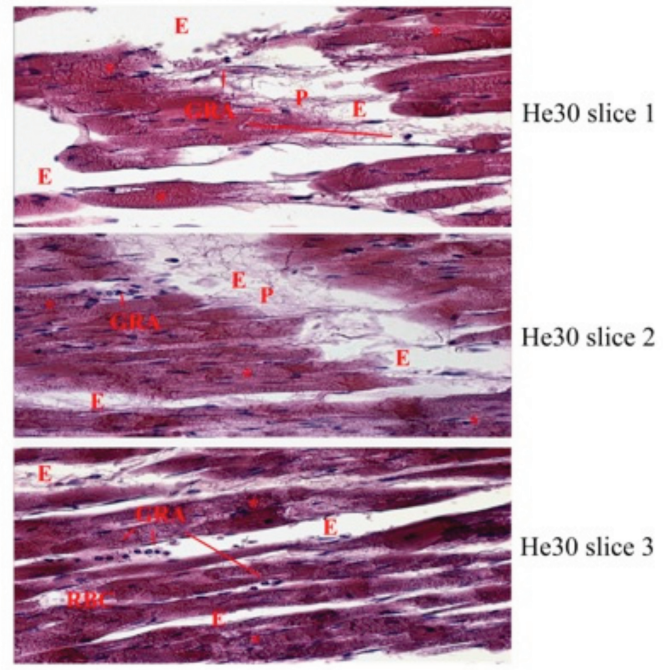

Supplementary Figure S10. Histology – He30. Representative slices of three animals that were exposed to 25 min of ischemia and 30 min of reperfusion with helium postconditioning for 30 min, 200 times enlarged. E indicates edema, RBC indicates extravasation of red blood cells, GRA indicates extravasation of granulocytes, P indicates presence of platelets and thrombi and asterisk indicates contraction band necrosis.

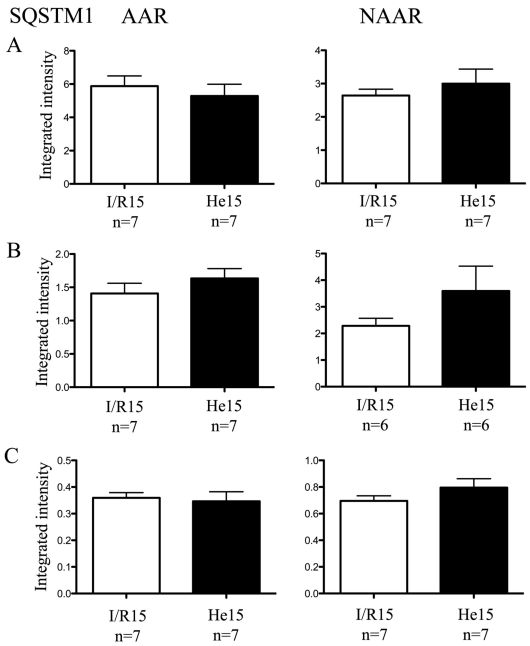

Supplementary Figure S11. Protein levels Sequestosome. Data are shown as mean +/- S.E.M. On the y-axis integrated intensity as (A) ratio of SQSTM/actin (cytosol fraction), (B) ratio of SQSTM/NaKATPase, (C) ratio of SQSTM/PHB1. AAR= area at risk, NAAR = rest of the myocardium, area not at risk.

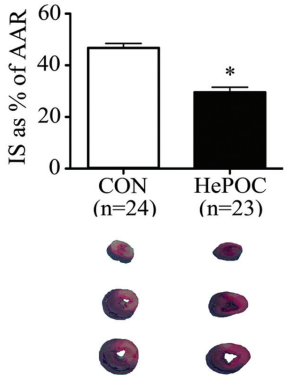

Supplementary Figure S12. Infarct sizes. Infarct sizes as percentage of area at risk. Data are plotted as mean ± S.E.M. * refers to statistical significance of HePOC vs CON. Below the graph, representative TTC-stained cross-sections of myocardium are shown for the control (CON) and 15-min HePOC group. Infarct sizes from 3 earlier studies (2,15,16) were compiled and analyzed using an unpaired Student *t* test.

REFERENCES

1 . Huhn R, Weber NC, Preckel B, Schlack W, Bauer I, *et al*. (2012) Age-related loss of cardiac preconditioning: impact of protein kinase A. *Exp Gerontol.* 47: 116-21.

2 . Huhn R, Heinen A, Weber NC, Kerindongo RP, Oei GT, *et al*. (2009) Helium-induced early preconditioning and postconditioning are abolished in obese Zucker rats in vivo. *J Pharmacol Exp Ther.* 329: 600-7.

3 . Heinen A, Huhn R, Smeele KM, Zuurbier CJ, Schlack W, *et al*. (2008) Helium-induced preconditioning in young and old rat heart: impact of mitochondrial Ca(2+) -sensitive potassium channel activation. *Anesthesiology.* 109: 830-6.

4 . Huhn R, Heinen A, Weber NC, Hieber S, Hollmann MW, *et al*. (2009) Helium-induced late preconditioning in the rat heart in vivo. *Br J Anaesth.* 102: 614-9.

5 . Pagel PS, Krolikowski JG. (2009) Transient metabolic alkalosis during early reperfusion abolishes helium preconditioning against myocardial infarction: restoration of cardioprotection by cyclosporin A in rabbits. *Anesth Analg.* 108: 1076-82.

6 . Pagel PS, Krolikowski JG, Amour J, Warltier DC, Weihrauch D. (2009) Morphine reduces the threshold of helium preconditioning against myocardial infarction: the role of opioid receptors in rabbits. *J Cardiothorac Vasc Anesth.* 23: 619-24.

7 . Pagel PS, Krolikowski JG, Shim YH, Venkatapuram S, Kersten JR, *et al*. (2007) Noble gases without anesthetic properties protect myocardium against infarction by activating prosurvival signaling kinases and inhibiting mitochondrial permeability transition in vivo. *Anesth Analg.* 105: 562-9.

8 . Pagel PS, Krolikowski JG, Pratt PF, Shim YH, Amour J, *et al*. (2008) Inhibition of glycogen synthase kinase or the apoptotic protein p53 lowers the threshold of helium cardioprotection in vivo: the role of mitochondrial permeability transition. *Anesth Analg.* 107: 769-75.

9 . Pagel PS, Krolikowski JG, Pratt PF, Shim YH, Amour J, *et al*. (2008) The mechanism of helium-induced preconditioning: a direct role for nitric oxide in rabbits. *Anesth Analg.* 107: 762-8.

10 . Pagel PS, Krolikowski JG, Pratt PF, Shim YH, Amour J, *et al*. (2008) Reactive oxygen species and mitochondrial adenosine triphosphate-regulated potassium channels mediate helium-induced preconditioning against myocardial infarction in vivo. *J Cardiothorac Vasc Anesth.* 22: 554-9.

11 . Saleem M, Qadir MI, Perveen N, Ahmad B, Saleem U, *et al*. (2013) Inhibitors Of Apoptotic Proteins: New Targets For Anti-Cancer Therapy. *Chem Biol Drug Des.* .

12 . Enari M, Sakahira H, Yokoyama H, Okawa K, Iwamatsu A, Nagata S. (1998) A caspase-activated DNase that degrades DNA during apoptosis, and its inhibitor ICAD. *Nature.* 391: 43-50.

13 . Lu X, Moore PG, Liu H, Schaefer S. (2011) Phosphorylation of ARC is a critical element in the antiapoptotic effect of anesthetic preconditioning. *Anesth Analg.* 112: 525-31.

14 . Bradford MM. (1976) A rapid and sensitive method for the quantitation of microgram quantities of protein utilizing the principle of protein-dye binding. *Anal Biochem.* 72: 248-54.

15. Oei GT, Hollmann MW, Preckel B, Weber NC. (2012) Cardioprotection after a short episode of 70% helium inhalation at early reperfusion is abrogated by prolonged inhalation during reperfusion. *American Society of Anesthesiologists.* Abstract A151.

16 . Oei GT, Huhn R, Heinen A, Hollmann MW, Schlack WS, *et al*. (2012) Helium-induced cardioprotection of healthy and hypertensive rat myocardium in vivo. *Eur J Pharmacol.* 684: 125-31.